AIP | Applied Physics Letters

Optical mobility of blood cells for label-free cell separation applications

Kyung Heon Lee, Kang Soo Lee, Jin Ho Jung, Cheong Bong Chang, and Hyung Jin Sung

Citation: Appl. Phys. Lett. **102**, 141911 (2013); doi: 10.1063/1.4801951
View online: http://dx.doi.org/10.1063/1.4801951
View Table of Contents: http://apl.aip.org/resource/1/APPLAB/v102/i14
Published by the AIP Publishing LLC.

Additional information on Appl. Phys. Lett.

Journal Homepage: http://apl.aip.org/
Journal Information: http://apl.aip.org/about/about_the_journal
Top downloads: http://apl.aip.org/features/most_downloaded
Information for Authors: http://apl.aip.org/authors

ADVERTISEMENT

Downloaded 06 Sep 2013 to 143.248.118.122. This article is copyrighted as indicated in the abstract. Reuse of AIP content is subject to the terms at: http://apl.aip.org/about/rights_and_permissions

Optical mobility of blood cells for label-free cell separation applications

Kyung Heon Lee, Kang Soo Lee, Jin Ho Jung, Cheong Bong Chang, and Hyung Jin Sung[a)]
Department of Mechanical Engineering, KAIST, 291 Daehak-ro, Yuseong-gu, Daejeon 305-701, South Korea

(Received 21 December 2012; accepted 1 April 2013; published online 12 April 2013)

This paper describes the optical mobilities of blood cell components. Blood cells are heterogeneous, and their optical behaviors depend on size, morphology, and other optical properties. In a step toward the label-free separation of blood cells, the optical mobility resulting from the optical scattering and cell properties was derived and evaluated for each cell component. The optical mobilities of red blood cells, lymphocytes, granulocytes, and monocytes were measured under various flow conditions of a cross-type optical particle separator. © *2013 AIP Publishing LLC* [http://dx.doi.org/10.1063/1.4801951]

Blood contains a tremendous amount of information about human body functions. Most blood components, including white blood cells (WBCs), red blood cells (RBCs), platelets, and plasma, can be used to assess the functions of tissues and organs in the human body. The clinical and biological analysis of body functions based on blood diagnostics requires blood cell component separation. Several well-developed techniques including flow cytometer, magnetic-activated cell sorting (MACS), fluorescence-activated cell sorting (FACS),[1,2] physical filteration,[3] and centrifugation[4] have been generally used in clinical and research field. Target cell isolation can require a labeling process, biomarker-conjugated micro-nano particles, or a media with a specific density. However, these methods require multi-step sample preparation, complex system, and labor-intensive process. Moreover, the introduction and removal of labeling materials can influence the characteristics of a cell, and the multi-step process can often cause target cell loss. The present lab-on-a-chip device is a simple and efficient label-free continuous separation method since microfluidics allows a precise control of blood cell separation in micro-scale environment. Several studies classified and isolated cells based on their biophysical properties, such as size differences,[5] deformability,[5,6] morphological differences,[7] density differences,[8] electric/magnetic susceptibilities,[9–11] and biochemical affinities;[12,13] however, the separation of cells based on their intrinsic properties remains a challenge.

Optical forces have been used as label-free techniques in a variety of fields. Optical forces are non-invasive in nature and yield high-precision controllability of micro- and nano-scale particles.[14–17] The optical tweezers can sort micro particles with a simple microstructure system. They can also sort bio samples by multiple parameters such as refractive index, size, shape, and fluorescence signal.[18–20] However, the optical tweezers use a relatively tightly focused beam spot, which can make latent damage on the cell, and they need some image processing process or optical actuator for spot manipulation. By contrast, the present cross-type optical particle separation (COPS)[21] uses the optical scattering force under a loosely focused beam so that the energy density on the spot is much smaller than that of the tightly focused beam of tweezers. The present device can work with simple optical components. In the present study, we measured the optical mobility in the context of a non-labeled continuous optical cell separation application.

In COPS, a laser beam is directed perpendicular to the direction of fluid flow so that the optical force shifts a micro-particle from its initial fluid streamline to other streamlines in the illumination region (Fig. 1). The distance between the initial and final streamlines, that is, the retention distance, is subject to mechanical and optical forces. By combining the optical force with the drag force due to the fluid flow, COPS can separate micron-sized particles successfully according to size, refractive index, or other structural characteristics.[21,22] The retention distance could be expressed as

$$z_r = K(m)\left(\frac{n_0 P d_p}{6cU\omega_0\pi\mu}\right), \tag{1}$$

where n_0 is the refractive index of media, P is the laser power, d_p is the diameter of the particle, c is the speed of light, ω_0 is the waist radius of the laser, μ is the dynamic viscosity of the fluid, and U is the fluid velocity. The dimensionless parameter K(m) represents the conversion efficiency

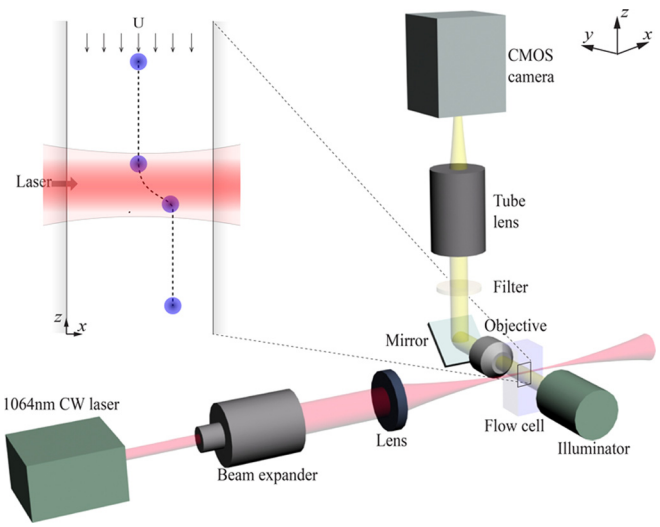

FIG. 1. A schematic diagram of the experimental setup.

[a)]Author to whom correspondence should be addressed. Electronic mail: hjsung@kaist.ac.kr.

 © 2013 AIP Publishing LLC

Downloaded 06 Sep 2013 to 143.248.118.122. This article is copyrighted as indicated in the abstract. Reuse of AIP content is subject to the terms at: http://apl.aip.org/about/rights_and_permissions

based on the photon momentum change during application of the scattering force.[21,22] For a standard single-layered particle, this efficiency depends on the relative refractive indices (m) of the particle. However, the photon momentum changes on the double-layered cell are affected by the scattering phenomena at each interface that $K(m)$ includes the morphology of the particle, e.g., non-spherical, disc-like micro-particles.

The optical behavior of cell in the COPS is different from standard micro particle. The heterogeneous characteristics of blood cell components make it difficult to predict their behaviors under optical forces; therefore, we employed the concept of optical mobility for real cell components. The optical mobility represents the characteristics resulting from optical scattering properties and the particle properties.[22] The optical mobility could be expressed in terms of the retention distance, the flow, and the laser conditions.

$$z_{opt} = \frac{d_p}{12\pi\mu} K(m) = z_r \left(\frac{cU\omega_0}{2n_0 P} \right). \quad (2)$$

Here, the optical mobility of a cell component can be obtained by measuring the retention distance when other conditions are fixed.

A polydimethylsiloxane (PDMS) microfluidic channel (200 μm in height and 700 μm in width) was designed to measure the cell behavior. The width of the channel was relatively large, yielding a negligible velocity profile difference around the channel center. Figure 1 shows a schematic diagram of the present cross-type optical cell separation. A PDMS micro-channel was used as the base material for the lab-on-a-chip device due to its simplicity and transmittance. The master mold structure was generated using SU8 photoresist (SU8-100, Microchem Corp., MA). Images were captured over a fixed focal plane, and a given initial velocity was used for data analysis to reduce the height directional position error for each cell.

Thermal damage to the cells under laser illumination was prevented by continuously illuminating a 1064 nm diode-pumped solid-state (DPSS) laser (Aptowave, USA). The absorption of laser to cell components, including HbO_2 in RBCs, was reliable with 1064 nm wavelength.[23] The laser was loosely focused into the microfluidic system using a 3× beam expander (Thorlabs, USA) and a 1 in. diameter, 100 mm focal length plano-convex lens (CVI, USA). Because laser illuminated in continuous fluid manner and loosely focused condition, the energy density of this system ($3.813 \times 10^3\ J^{-2}$) was much lower than those of other optical tweezer and other optical force based sorting devices.[17,18] High-precision syringe pumps (Cetoni GmbH, Germany) were provided to control the fluid flow through the microchannel. The microchannel was mounted on a custom-built multi-axis stage to facilitate precise alignment. Images were collected through a 20× objective lens (Olympus, Japan), a low-pass filter, and a high-speed camera (PCO, Germany).

The high concentration of RBCs in a 1 mM of ethylenediaminetetraacetic acid (EDTA) solution was reduced using the conventional RBCs lysis procedures using ammonium chloride-potassium (ACK) buffer prior to cell sorting. The cells were separated through a flow cytometer (Becton Dickinson, Aria II). In the present study, blood cell components were prepared with four component; i.e., RBCs, lymphocytes, granulocytes, and monocytes. Performing the whole experimental procedure within a day of the isolation process maximized the viability of blood cell components.

Two polystyrene latex (PSL) particle sizes (Duke scientific, $d_p = 5\ \mu$m, 10 μm) were used as a calibration reference for the system. The 1064 nm laser was invisible; therefore, it was particularly crucial to align the laser in the channel with care. The laser was aligned perpendicular to the fluid flow using our previous theoretical and experimental retention distances derived for standard PSL particles.[21] The experimental measurements and theoretical calculations based on the standard PSL particles were compared prior to each cell component measurement.

Isolated human blood cell components were used to measure the behaviors of each component in the COPS. Figure 2 shows the captured trajectories of cell components; i.e., RBC (a), lymphocyte (b), granulocyte (c), and monocyte (d). The inset of each figure shows the microscopic image of each cell component. Before the blood cell components flowed into the laser illumination region, the blood cell components moved along the streamlines of the fluid flow. As the blood components moved into the laser illumination region, the optical scattering force repelled the blood cells away from their original streamlines. The laser illumination was directed perpendicular to the fluid flow; therefore, the blood cell components moved along the vertical direction of fluid flow under the optical scattering force. The vertical distance between the initial and final positions of the blood cell component was defined as the retention distance. The retention distances of RBCs were the largest among the blood cell components, and the monocytes yielded the highest value among the WBCs. The average monocyte size (mean diameter: $12.5 \pm 1.4\ \mu$m) exceeded the size of the granulocytes (mean diameter: $10.9 \pm 1.5\ \mu$m) and the lymphocytes (mean diameter: $9.0 \pm 1.1\ \mu$m); therefore, the monocyte retention distance exceeded the retention distances of the other WBCs components. For RBCs, shape was an important parameter. Although the RBC size (mean diameter: $5.9 \pm 1.1\ \mu$m) was

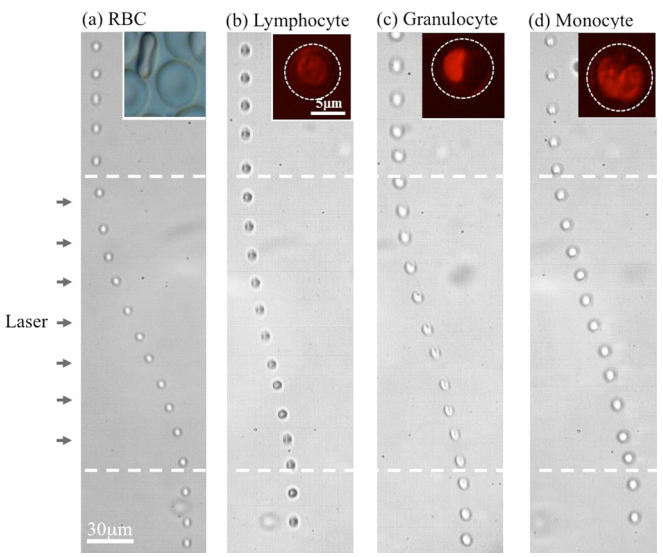

FIG. 2. Snapshots of the cell trajectories for (a) RBCs, (b) lymphocytes, (c) granulocytes, and (d) monocytes.

Downloaded 06 Sep 2013 to 143.248.118.122. This article is copyrighted as indicated in the abstract. Reuse of AIP content is subject to the terms at: http://apl.aip.org/about/rights_and_permissions

much smaller than that of the WBCs, the RBC retention distance exceeded that of the WBCs.

The retention distance of each cell component was measured under the 3 W laser power and several fluid flow conditions. The results are shown in Fig. 3. The retention distance of each cell increased linearly with the flow velocity, and the retention distance difference increased. The gradient force was negligible at this laser power and under these flow velocity conditions. The retention distances of the RBCs were the largest of all cell components, and the monocytes yielded the largest values among the WBCs components. We confirmed that the retention distances of RBCs were always larger than those of the WBCs. The disc-like RBC shape altered the photon stream relative to that of the WBCs or other spherical micro-particles. By contrast, the incident angle was considered for the non-spherical particles. The scattering parameter $K(m)$ for a disc-like shape was higher than that of a spherical shape. Because the width and height of the microfluidic channel (width: 700 μm and height: 200 μm) are much larger than the diameter of blood cells (diameter: 5–12 μm), we found that the velocity profile at the center of the channel is uniform. Most of cells in COPS are flowing with a very low Reynolds number through the center region of the channel. As shown in Fig. 1, the plane of shear is normal to the channel height, and the main axis of the cell is parallel to the shear plane.[24,25] This means that the rotation of the cell by the optical force is very small. The size of each component and the structural heterogeneity of WBCs were another important parameter that influenced the retention distance. For example, the retention distance of a double-layered spherical structure may be a function of the size and the optical properties of the inner spherical structure.[26] As shown in the inset of Fig. 2, the monocytes and granulocytes are larger than lymphocytes and have relatively complex inner structures than that of lymphocytes. The retention distances of those two cells are larger than that of lymphocytes.

The size and structural heterogeneity among the blood cell components made it difficult to predict the behavior of the blood components in a theoretical way; however, the retention distance results shown in Fig. 3 indicated that each component yielded distinct optical behaviors in COPS. The

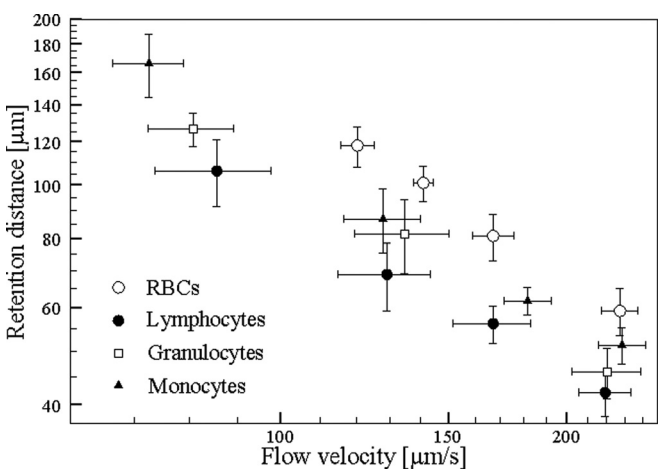

FIG. 3. Retention distance of the blood cell components in the COPS.

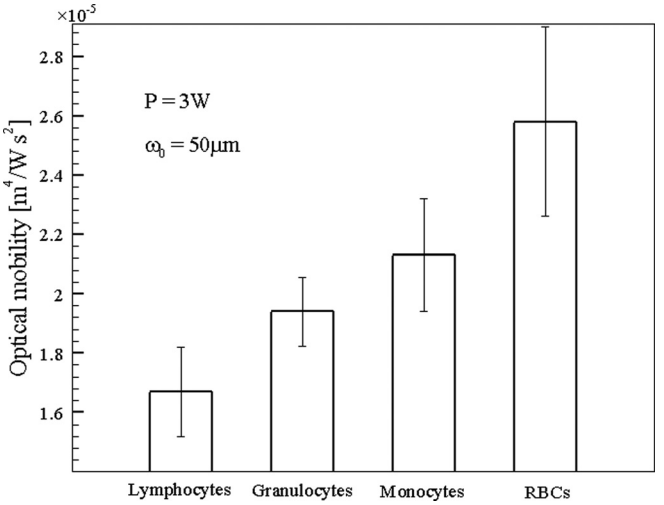

FIG. 4. Optical mobilities of lymphocytes (N = 59), granulocytes (N = 36), monocytes (N = 42), and RBCs (N = 81). Error bars represent the standard deviations across each cell population.

optical mobility, which was composed of the efficiency of the scattering force and the material properties, could be used to overcome the structural complexity of each cellular component. As shown in Eq. (2), the optical mobility could be expressed in terms of the retention distance, the flow, and the laser conditions. Despite the sample heterogeneity, the optical behaviors could be predicted using the instrumental parameters, including the flow velocity (U), laser power (P), laser beam waist radius (ω_0), and refractive index of the outer media (n_0). The laser beam waist radius was fixed at $\omega_0 = 50$ μm, and the 3 W laser was used. Figure 4 shows the optical mobility of each cell component. The error bar indicates the standard deviations of the measured data. The trend in the optical mobilities mirrored the flow velocity for each cell component. RBCs had the largest optical mobilities among the blood cell components. Among WBCs, the monocytes yielded the largest optical mobilities, and the lymphocytes yielded the smallest optical mobilities. The granulocytes produced more scattering than other WBC components, and the optical trapping force on the granulocytes was the largest[18] among WBCs. Table I shows the optical mobilities of the blood cell components and standard particles.[22] Because of optical mobilities including morphologies and material properties, while the refractive index and diameter of RBCs are similar to those of silica particles,[22] the optical mobility of RBCs is about 3 times larger than that of silica particles.

TABLE I. Properties of the blood cell components and standard particles.

	Mean diameter (μm)	Optical mobility (m^4/Ws^2)
RBCs	5.9 ± 1.1	2.58×10^{-5} ($\pm 0.32 \times 10^{-6}$)
Lymphocytes	9.0 ± 1.1	1.67×10^{-5} ($\pm 0.15 \times 10^{-6}$)
Monocytes	12.5 ± 1.4	2.13×10^{-5} ($\pm 0.19 \times 10^{-6}$)
Granulocytes	10.9 ± 1.5	1.94×10^{-5} ($\pm 0.12 \times 10^{-6}$)
PSL[22]	10.0 ± 0.1	5.16×10^{-5}
PSL[22]	5.0 ± 0.1	2.58×10^{-5}
Silica[22]	4.8 ± 0.4	0.80×10^{-5}

Downloaded 06 Sep 2013 to 143.248.118.122. This article is copyrighted as indicated in the abstract. Reuse of AIP content is subject to the terms at: http://apl.aip.org/about/rights_and_permissions

The present study measured the optical mobilities of blood cells in COPS. The shape irregularities of the cellular components guided us to measure the optical mobility, which includes the scattering characteristic of a cell and is derived in terms of the retention distance. The optical mobilities of four components of blood cells were measured, including RBCs, lymphocytes, granulocytes, and monocytes. The optical mobilities of the RBCs were quite large because of their disc-like shapes. Each WBC component also yielded a distinct optical mobility. The optical mobility can be used for label-free separation and detection of blood cell behaviors.

This work was supported by the Creative Research Initiatives (No. 2012-0000246) program of the National Research Foundation of Korea.

[1]M. Toner and D. Irimia, Annu. Rev. Biomed. Eng. **7**, 77 (2005).
[2]W. A. Bonner, H. R. Hulett, R. G. Sweet, and L. A. Herzenberg, Rev. Sci. Instrum. **43**, 404 (1972).
[3]T. A. Crowley and V. Pizziconi, Lab Chip **5**, 922 (2005).
[4]A. Bøyum, Scand. J. Immunol. **5**, 9 (1976).
[5]J. P. Beech, S. H. Holm, K. Adolfsson, and J. O. Tegenfeldt, Lab Chip **12**, 1048 (2012).
[6]H. Bow, I. V. Pivkin, M. Diez-Silva, S. J. Goldfless, M. Dao, J. C. Niles, S. Suresh, and J. Han, Lab Chip **11**, 1065 (2011).
[7]M. Chabert and J. L. Viovy, Proc. Natl. Acad. Sci. U.S.A. **105**, 3191 (2008).
[8]M. Godin, F. F. Delgado, S. M. Son, W. H. Grover, A. K. Bryan, A. Tzur, P. Jorgensen, K. Payer, A. D. Grossman, M. W. Kirschner, and S. R. Manalis, Nat. Methods **7**, 387 (2010).
[9]S. I. Han, S. M. Lee, Y. D. Joo, and K. H. Han, Lab Chip **11**, 3864 (2011).
[10]F. Shen, H. Hwang, Y. K. Hahn, and J. K. Park, Anal. Chem. **84**, 3075 (2012).
[11]U. Kim, C. W. Shu, K. Y. Dane, P. S. Daugherty, J. Y. J. Wang, and H. Soh, Proc. Natl. Acad. Sci. U.S.A. **104**, 20708 (2007).
[12]S. Nagrath, L. V. Sequist, S. Maheswaran, D. W. Bell, D. Irimia, L. Ulkus, M. R. Smith, E. L. Kwak, S. Digumarthy, A. Muzikansky, P. Ryan, U. J. Balis, R. G. Tompkins, D. A. Haber, and M. Toner, Nature (London) **450**, 1235 (2007).
[13]S. Choi, J. M. Karp, and R. Karnik, Lab Chip **12**, 1427 (2012).
[14]A. H. J. Yang, S. D. Moore, B. S. Schmidt, M. Klug, M. Lipson, and D. Erickson, Nature (London) **457**, 71 (2009).
[15]A. Ashkin, Phys. Rev. Lett. **24**, 156 (1970).
[16]M. P. MacDonald, G. C. Spalding, and K. Dholakia, Nature (London) **426**, 421 (2003).
[17]M. M. Wang, E. Tu, D. E. Raymond, J. M. Yang, H. Zhang, N. Hagen, B. Dees, E. M. Mercer, A. H. Forster, I. Kariv, P. J. Marchand, and W. F. Butler, Nat. Biotechnol. **23**, 83 (2005).
[18]C. G. Hebert, A. Terray, and S. J. Hart, Anal. Chem. **83**, 5666 (2011).
[19]B. Landenberger, H. Hofemann, S. Wadle, and A. Rohrbach, Lab Chip **12**, 3177 (2012).
[20]M. Werner, F. Merenda, J. Piguet, R.-P. Salathé, and H. Vogel, Lab Chip **11**, 2432 (2011).
[21]S. B. Kim, S. Y. Yoon, H. J. Sung, and S. S. Kim, Anal. Chem. **80**, 2628 (2008).
[22]S. B. Kim, E. Jung, H. J. Sung, and S. S. Kim, Appl. Phys. Lett. **93**, 044103 (2008).
[23]K. Svoboda and S. M. Block, Annu. Rev. Biophys. Biomol. Struct. **23**, 247 (1994).
[24]T. M. Fischer, M. Stohr-Lissen, and H. Schmid-Schonbein, Science **202**, 894 (1978).
[25]M. Abkarian, M. Faivre, and A. Viallat, Phys. Rev. Lett. **98**, 188302 (2007).
[26]K. H. Lee, S. B. Kim, S. Y. Yoon, K. S. Lee, J. H. Jung, and H. J. Sung, Langmuir **28**, 7343 (2012).

Downloaded 06 Sep 2013 to 143.248.118.122. This article is copyrighted as indicated in the abstract. Reuse of AIP content is subject to the terms at: http://apl.aip.org/about/rights_and_permissions